

Modulating carrier and sideband coupling strengths in a standing wave gate beam

Thomas E. deLaubenfels,^{1,2} Karl A. Burkhardt,^{3,*} Grahame Vittorini,^{2,†}

J. True Merrill,¹ Kenneth R. Brown,^{3,2,4} and Jason M. Amini¹

¹Georgia Tech Research Institute, Atlanta, GA 30332, USA

²School of Physics, Georgia Institute of Technology, Atlanta, GA 30332, USA

³School of Chemistry and Biochemistry, Georgia Institute of Technology, Atlanta, GA 30332, USA

⁴School of Computational Science and Engineering,

Georgia Institute of Technology, Atlanta, GA 30332, USA

(Dated: August 30, 2022)

We control the relative coupling strength of carrier and first order motional sideband interactions of a trapped ion by placing it in a resonant optical standing wave. Our configuration uses the surface of a microfabricated chip trap as a mirror, avoiding technical challenges of in-vacuum optical cavities. Displacing the ion along the standing wave, we show a periodic suppression of the carrier and sideband transitions with the cycles for the two cases 180° out of phase with each other. This technique allows for suppression of off-resonant carrier excitations when addressing the motional sidebands, with applications in quantum simulation and quantum control. Using the standing wave fringes, we measure the relative ion height as a function of applied electric field, allowing for a precise measurement of ion displacement and, combined with measured micromotion amplitudes, a validation of trap numerical models.

PACS numbers: 03.67.Lx, 32.80.Qk, 37.10.Ty

The excitation spectrum of a trapped ion in a radio frequency (RF) trap acquires sidebands due to the harmonic motion of the ion [1]. This leads to an almost ideal Jaynes-Cummings interaction [2, 3] which couples the internal degrees of freedom to the ion motion and is the basis for two-qubit gates in ion trap quantum computation [4–6]. If the optical field is a standing wave, the coupling strengths of the carrier and sidebands acquire a periodic dependence on the atom’s spatial position within the standing wave fringes [7, 8] with the cycles for the two cases 180° out of phase with each other. This dependence has been demonstrated in cavity experiments with trapped ions [1, 9, 10]. However, the use of cavities involves technical challenges, in particular when integrating the cavity with microfabricated ion traps where optics and dielectric mirrors can become charged [11, 12].

In this paper, we demonstrate the same position dependence with a single mirror which, in this case, is simply the surface of the ion trap itself (Fig. 1). To handle the case of imperfect beam alignment, reflection losses, and similar system limitations, we extend the calculations of Refs. [7, 8] to the case of non-normal incidence laser beams and unequal couplings of the incident and reflected laser beams with the ion. We find a criterion for the out of phase carrier and sideband coupling strengths that is set by the incident angle of the laser beam and the orientation of the ion’s harmonic motion.

Replacing running wave optical beams with standing wave beams provides a method to reduce off-resonant carrier excitations when addressing the motional sidebands [7, 13]. Sideband interactions are used widely in trapped ion experiments for a variety of functions such as cooling to the motional ground state [14], measurements of the ion heating rate [15, 16], identifying and cooling molec-

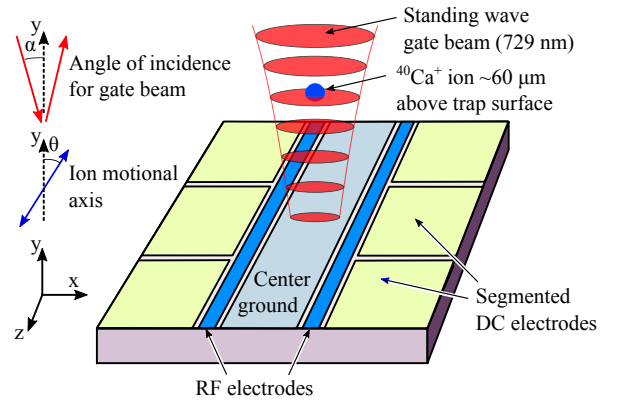


FIG. 1. Schematic of the experimental configuration. $^{40}\text{Ca}^+$ ions are confined $\sim 60 \mu\text{m}$ above the trap surface by RF and DC electric fields. 729 nm light is used to excite the $|S_{1/2}, m_F = -\frac{1}{2}\rangle \rightarrow |D_{5/2}, m_F = -\frac{5}{2}\rangle$ quadrupole transition. The incident 729 nm laser (with incidence angle α) is retro-reflected from the aluminum trap surface to produce a standing wave. The ion is displaced through the standing wave fringes by changing the trap fields.

ular ions [17–19], and implementing entangling gates [4–6]. Off-resonant coupling to the carrier, either evident as motion independent population transfer or an AC Stark shift, places a limit on the speed of the sideband interactions. Suppressing the carrier can remove this limit and, in particular, would allow for improved two-qubit gate fidelities as the gate time becomes comparable or shorter than a cycle of the harmonic motion [5, 20].

Suppression of the carrier transition also has applications in quantum simulation. Trapped ions have been

proposed as a system for modeling the expansion of the universe [21]. The simulation requires off-resonant excitation of both the red and blue sidebands by a red-detuned exciting field, with no coupling to the carrier. Because the blue sideband is both weaker and further from resonance than the carrier transition, suppression of the carrier is important for such an experiment.

A trapped ion interacting with an ideal standing wave laser field is treated in Refs. [7, 8]. We extend this treatment to include an angle of incidence α relative to the mirror normal (see Fig. 1) and differing couplings of the incident and reflecting beams to the atomic transition. The latter can arise due to imperfect reflectivity of the mirror, differing polarization of the two beams, and, for quadrupole transitions such as used here, the laser beam k vector dependence of the coupling. For a harmonically trapped two level atom in the rotating wave approximation, the interaction Hamiltonian (up to a global phase) is

$$\begin{aligned} \hat{H}_I = & \frac{\hbar}{2} \hat{\sigma}_+ e^{-i\Delta t} \\ & \times \left\{ \Omega_1 \exp \left[-i\gamma + i\eta_1(\hat{a}e^{i\nu t} + \hat{a}^\dagger e^{-i\nu t}) \right] \right. \\ & \left. + \Omega_2 \exp \left[i\gamma + i\eta_2(\hat{a}e^{i\nu t} + \hat{a}^\dagger e^{-i\nu t}) \right] \right\} + \text{h.c.} \end{aligned}$$

Here, Ω_1 and Ω_2 are the Rabi frequencies of the incident and reflected beams, respectively, $\hat{\sigma}_+$ ($\hat{\sigma}_-$) is the raising (lowering) operator of the two level atom, \hat{a}^\dagger (\hat{a}) is the raising (lowering) operator of the secular motion, $\Delta = \omega_{laser} - \omega_0$ is the laser's detuning from the carrier resonance, and ν is the secular frequency. The phase $\gamma = ky \cos \alpha + \phi/2$, where y is the atom's equilibrium position and ϕ is the relative phase between the coupling coefficients of the incident and reflected laser fields. When the laser field is at near-normal incidence, the phase $\phi = 0$ ($= \pi$) for a quadrupole (dipole) transition. In this case, $\gamma = l\pi$, for integer l , corresponds to a node (anti-node) in the standing wave. The Lamb-Dicke parameters η_1 and η_2 are defined as

$$\eta_j = k \sqrt{\frac{\hbar}{2m\nu}} \left[\sin \theta \sin \alpha + (-1)^j \cos \theta \cos \alpha \right]$$

where θ is the angle of the motional mode axis relative to surface normal, m is the ion mass, and k is the wavenumber of the gate beam.

In the Lamb-Dicke approximation, the interaction Hamiltonian can be decomposed into a carrier term

$$\begin{aligned} \hat{H}_{car} = & \frac{\hbar}{2} \hat{\sigma}_+ e^{-i\Delta t} \\ & \times \left\{ \Omega_1 \left[1 - \frac{\eta_1^2}{2} (1 + 2\hat{a}^\dagger \hat{a}) \right] e^{-i\gamma} \right. \\ & \left. + \Omega_2 \left[1 - \frac{\eta_2^2}{2} (1 + 2\hat{a}^\dagger \hat{a}) \right] e^{i\gamma} \right\} + \text{h.c.}, \end{aligned}$$

a red sideband term

$$\begin{aligned} \hat{H}_{rsb} = & \frac{i\hbar}{2} \hat{\sigma}_+ \hat{a} e^{-i(\Delta+\nu)t} (\Omega_1 \eta_1 e^{-i\gamma} + \Omega_2 \eta_2 e^{i\gamma}) \\ & + \text{h.c.}, \end{aligned}$$

and a corresponding blue sideband term. Following the treatment in Ref. [22], these Hamiltonians lead to respective coupling strengths

$$\begin{aligned} \Omega_{car} = & \Omega_1 e^{-i\gamma} \left[1 - \frac{\eta_1^2}{2} (1 + 2n) \right] \\ & + \Omega_2 e^{i\gamma} \left[1 - \frac{\eta_2^2}{2} (1 + 2n) \right] \end{aligned} \quad (1)$$

and

$$\begin{aligned} \Omega_{rsb} = & i\sqrt{n} (\Omega_1 e^{-i\gamma} \eta_1 + \Omega_2 e^{i\gamma} \eta_2) \\ \Omega_{bsb} = & i\sqrt{n+1} (\Omega_1 e^{-i\gamma} \eta_1 + \Omega_2 e^{i\gamma} \eta_2) \end{aligned} \quad (2)$$

where n is the occupation number of the quantized harmonic oscillator. Interference between the $e^{\pm i\gamma}$ terms produce fringes in the coupling strengths as the ion position changes. When $\cos \theta \cos \alpha > \sin \theta \sin \alpha$, η_1 and η_2 have opposite signs, and the carrier and sideband fringes are 180° out of phase.

For $\gamma = l\pi$ (with l an integer), the carrier coupling strength is maximized while the sideband coupling strengths are minimized. For $\gamma = (l + 1/2)\pi$, the converse is true. These fringes correspond to a physical displacement of the ion by $y = \lambda/(2 \cos \alpha)$, where λ is the wavelength of the exciting laser.

Our experimental configuration is depicted schematically in Fig. 1. We use a surface electrode linear ion trap to confine and cool $^{40}\text{Ca}^+$ ions, as described in Ref. [23]. The ion is confined $\sim 60 \mu\text{m}$ above the trap surface by a combination of RF and DC potentials. We use the $|S_{1/2}, m_F = -\frac{1}{2}\rangle \rightarrow |D_{5/2}, m_F = -\frac{5}{2}\rangle$ quadrupole transition at $\lambda = 729 \text{ nm}$ for our measurements. The 729 nm beam reflects off of the aluminum trap surface with a reflectivity of 86%, producing a standing wave field in the y direction. the angle $|\alpha| \approx 20^\circ$ due to restrictions in the beam path, which limits the fringe contrast. We tune the laser to address the carrier transition or to address the first order red sideband transition of a motional mode with $\nu = 4.75 \text{ MHz}$ (on the RF null) and $\theta = 13^\circ$ (see Fig. 1).

To displace the ion's equilibrium position along the standing wave, we apply an electric field E_y by adjusting the trap's DC potentials. The case $E_y = 0$ corresponds to the ion being on the RF null. For $E_y > 0$ and $E_y < 0$, the ion is displaced along $+y$ and $-y$, respectively. The range of E_y values used in this experiment displaces the ion over a $10 \mu\text{m}$ range. The fringes in the carrier and sideband transitions resulting from this displacement are evident in Fig. 2.

Displacing the ion from its equilibrium position on the RF null affects the dynamics in several ways beyond the

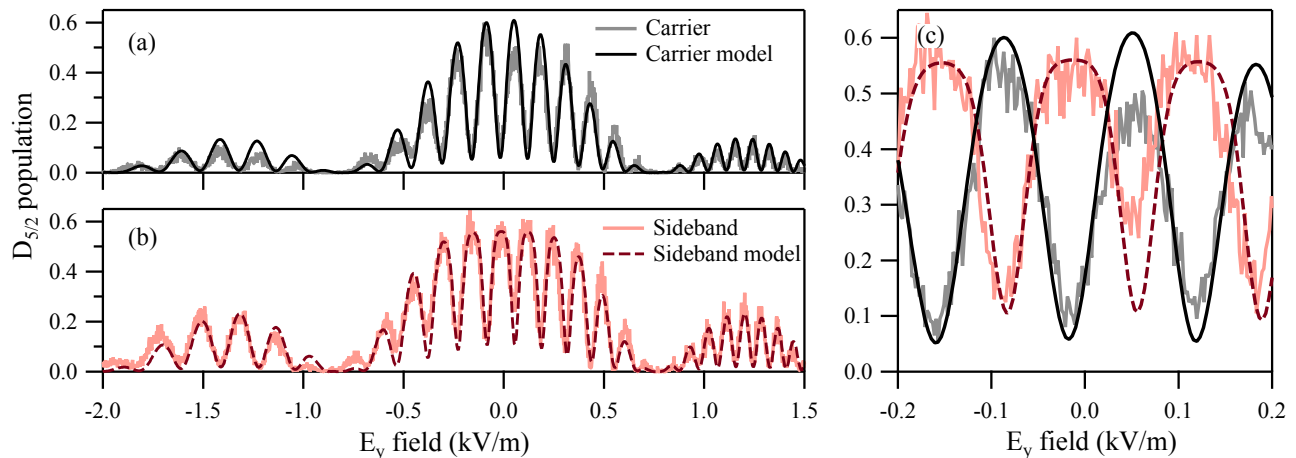


FIG. 2. $D_{5/2}$ populations vs. applied E_y field measured after (a) carrier and (b) red sideband transitions. The sideband's gate beam power is 9.5 dB greater than the carrier's, and the interaction time is fixed for both cases (13 μ s). The overall envelope is generated by the micromotion modulation $J_0(\kappa)$ (see text). (c) The carrier and sideband populations oscillate 180° out of phase as the ion is transported through the standing wave fringes. The solid lines represent a fit to the data using the model described in the text. The deviation between the data and fit at $E_y \approx 0.05$ kV/m may be due to scattering of the reflected light from the trap surface.

fringing. First, the displacement introduces micromotion [24] that modulates the coupling strengths of both the carrier and sideband [25]. To account for this modulation, we multiply equations (1) and (2) by the Bessel function $J_0(\kappa)$, where κ is the modulation parameter given by

$$\kappa = \cos \beta \frac{2}{\lambda \nu_{RF}} \sqrt{\frac{q \Phi_{pp}(x, y)}{m}}. \quad (3)$$

Here λ is the wavelength of the gate beam, ν_{RF} is the trap RF frequency, m and q are the mass and charge of the ion, respectively, $\Phi_{pp}(x, y)$ is the RF pseudopotential, and β is the angle between the micromotion direction and the gate beam. Our trap has an RF quadrupole that is rotated in the xy plane relative to the surface normal [23]; during ion displacement, we apply a small E_x proportional to E_y such that $\beta = 0$ at all points. Second, the ion's motional frequencies change after displacement. We track the changing frequency by measuring the sideband's resonance for different displacements.

Figures 2(a) and (b) show $D_{5/2}$ state populations measured after driving carrier or sideband transitions as a function of applied E_y field. We observe fringes due to the standing wave field superimposed with the $J_0(\kappa)$ envelope due to the micromotion modulation. The maxima (minima) of the carrier fringes correspond to the ion positioned on nodes (anti-nodes) of the standing wave. The carrier and sideband fringes are overlaid in Fig. 2(c). The standing wave fringes of the carrier and sideband oscillate 180° out of phase with one another, as predicted by equations (1) and (2).

Figures 3(a) shows that by adjusting the ion's position in the standing wave laser field, we can achieve an ef-

fective suppression of the carrier that is equivalent to an 8 dB reduction in the gate beam power. For the sideband in Fig. 3(b), an equivalent 11 dB reduction can be achieved.

To produce the fits seen in Figs. 2 and 3, we use the excited state population equation for a thermal ion given by

$$P(D_{5/2}) = \sum_{n=0}^{\infty} \frac{\bar{n}^n}{(\bar{n} + 1)^{n+1}} \sin^2 \left[\frac{1}{4} \Omega(\gamma, n) J_0(\kappa) t \right],$$

where \bar{n} is the ion's mean number of motional quanta and $\Omega(\gamma, n)$ is Ω_{car} or Ω_{rsb} depending on whether we are fitting carrier or sideband data, respectively [24]. The fringes and overall envelope in Fig. 2 arise from the dependence of γ and κ on the ion's displacement y . We parametrize $\gamma = ky \cos \alpha$ with $y = \sum_{j=0}^4 a_j E_y^j$ and parametrize $\kappa^2 = \sum_{j=2}^4 m_j E_y^j$, for coefficients a_j and m_j . These coefficients, along with Ω_1 , Ω_2 , α , and \bar{n} , form the full set of parameters that define the simultaneous fits of the data in Figs. 2 and 3. In particular, the set has $|\alpha| = 18^\circ$, $\Omega_2 / \Omega_1 = 0.52$, and $\bar{n} = 18$.

Using equation (3), we can determine the pseudopotential Φ_{pp} from κ^2 . Fig. 4 plots the resulting Φ_{pp} and the ion displacement y as a function of E_y . We compare these with the results from a numerical model of the trapping potentials. The model includes a 700 V/m uniform stray field that was adjusted to match the observed RF null in Fig. 2. The magnitude of the RF trapping potential used in the model was adjusted to match the observed mode frequencies at $E_y = 0$. There are no other free parameters used in the model. The agreement seen provides a measure of confidence in the model and future

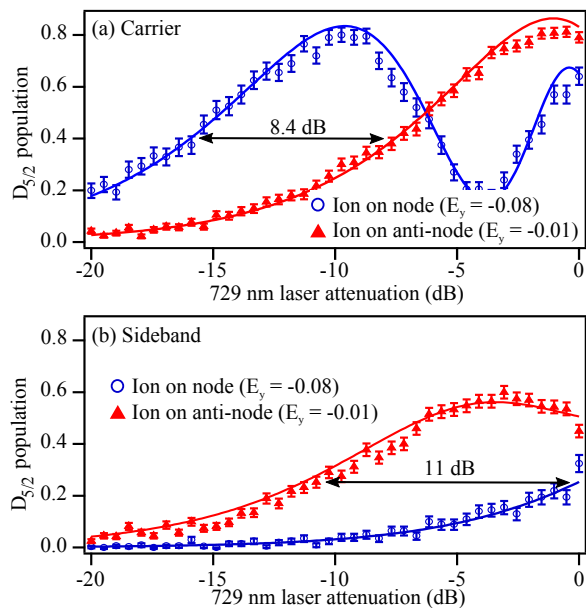


FIG. 3. $D_{5/2}$ populations vs. relative gate beam power measured after (a) carrier and (b) red sideband transitions. Interaction time is fixed for both cases ($13 \mu\text{s}$). The populations were measured with the ion on either a node (blue circles) or an adjacent anti-node (red triangles) near the RF null ($J_0(\kappa) \approx 1$). An effective suppression of 8 dB for the carrier and 11 dB for the sideband is achieved. The solid lines represent a simultaneous fit to the data using the model described in the text. The results from Fig. 2(a) and (b) were acquired at -13.5 dB and -4 dB, respectively.

predictions.

In conclusion, we have demonstrated how the carrier and motional sideband transition coupling strengths of a trapped ion may be controlled by displacing the ion within a resonant standing wave field. In our configuration, in which a standing wave is formed by retro-reflecting an incident beam off of a surface electrode trap, we achieve suppression of the carrier (sideband) by the equivalent of an 8 dB (11 dB) reduction in the driving beam power. The suppression achievable ultimately depends on the quality of the standing wave field at the ion's position, which is related to the ratio Ω_2/Ω_1 . The trap's surface reflectivity limits us here to $\Omega_2/\Omega_1 = \sqrt{0.86} = 0.93$. We can approach this limit with improved beam alignment, which would allow for a carrier suppression equivalent to a 29 dB reduction in driving beam power when $\bar{n} \approx 0$ and $|\alpha| < 10^\circ$. This reaches the regime in which modeling the expansion of the universe with trapped ions becomes experimentally feasible [21]. Further suppression would require the use of a more reflective surface. We measure the reflectivity from a gold coated trap like the one described Ref. [26] to be $> 98\%$, which could provide an equivalent carrier suppression of > 40 dB. Similar quality standing waves could be gener-

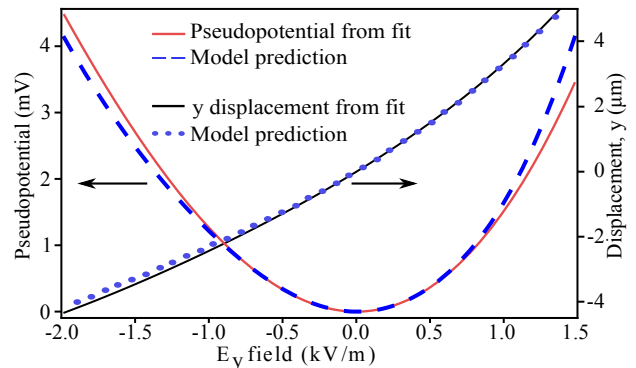


FIG. 4. Dependence of the pseudopotential Φ_{pp} and ion displacement y on the applied field E_y , along with predictions from a numerical model of the trapping potentials. Deviations from the model can be attributed non-uniformity of the stray fields in the trapping region.

ated by incorporating a metallic mirror adjacent to an ion trap if the trap surface is not amenable to this purpose.

This work was supported by the Georgia Tech Research Institute. KRB was supported by the Director of National Intelligence (ODNI), Intelligence Advanced Research Projects Activity (IARPA), under US Army Research Office (ARO) contracts W911NF-10-1-0231. TD would like to thank support by a Georgia Tech President's Fellowship.

* Current address: Department of Physics, University of Texas at Austin, Austin, TX 78712, USA

† Current address: Honeywell International, Golden Valley, MN 55422, USA

- [1] D. R. Leibrandt, J. Labaziewicz, V. Vuletić, and I. L. Chuang, *Phys. Rev. Lett.* **103**, 103001 (2009).
- [2] E. T. Jaynes and F. W. Cummings, *Proc. of the IEEE* **51**, 89 (1963).
- [3] Y. Wu and X. Yang, *Phys. Rev. Lett.* **78**, 3086 (1997).
- [4] J. I. Cirac and P. Zoller, *Phys. Rev. Lett.* **74**, 4091 (1995).
- [5] A. Sørensen and K. Mølmer, *Phys. Rev. A* **62**, 022311 (2000).
- [6] F. Schmidt-Kaler, H. Häffner, M. Riebe, S. Gulde, G. P. Lancaster, T. Deuschle, C. Becher, C. F. Roos, J. Eschner, and R. Blatt, *Nature* **422**, 408 (2003).
- [7] J. I. Cirac, R. Blatt, P. Zoller, and W. D. Phillips, *Phys. Rev. A* **46**, 2668 (1992).
- [8] D. F. V. James, *Appl. Phys. B* **66**, 181 (1998).
- [9] G. Guthöhrlein, M. Keller, K. Hayasaka, W. Lange, and H. Walther, *Nature* **414**, 49 (2001).
- [10] M. Steiner, H. M. Meyer, C. Deutsch, J. Reichel, and M. Köhl, *Phys. Rev. Lett.* **110**, 043003 (2013).
- [11] M. Harlander, M. Brownnutt, W. Hnsel, and R. Blatt, *New J. Phys.* **12**, 093035 (2010).
- [12] C. R. Clark, C.-w. Chou, A. R. Ellis, J. Hunker, S. A. Kemme, P. Maunz, B. Tabakov, C. Tigges, and D. L.

- Stick, *Phys. Rev. Appl.* **1**, 024004 (2014).
- [13] S. Zhang, C.-W. Wu, and P.-X. Chen, *Phys. Rev. A* **85**, 053420 (2012).
- [14] F. Diedrich, J. C. Bergquist, W. M. Itano, and D. J. Wineland, *Phys. Rev. Lett.* **62**, 403 (1989).
- [15] Q. A. Turchette, Kielpinski, B. E. King, D. Leibfried, D. M. Meekhof, C. J. Myatt, M. A. Rowe, C. A. Sackett, C. S. Wood, W. M. Itano, C. Monroe, and D. J. Wineland, *Phys. Rev. A* **61**, 063418 (2000).
- [16] G. Shu, G. Vittorini, A. Buikema, C. S. Nichols, C. Volin, D. Stick, and K. R. Brown, *Phys. Rev. A* **89**, 062308 (2014).
- [17] J. E. Goeters, C. R. Clark, G. Vittorini, K. Wright, C. R. Viteri, and K. R. Brown, *J. Phys. Chem. A* **117**, 9725 (2013).
- [18] R. Rugango, J. E. Goeters, T. H. Dixon, J. M. Gray, N. B. Khanyile, G. Shu, R. J. Clark, and K. R. Brown, *New J. Phys.* **17**, 035009 (2015).
- [19] Y. Wan, F. Gebert, F. Wolf, and P. O. Schmidt, *Phys. Rev. A* **91**, 043425 (2015).
- [20] J. Mizrahi, B. Neyenhuis, K. Johnson, W. Campbell, C. Senko, D. Hayes, and C. Monroe, *Appl. Phys. B* **114**, 45 (2014).
- [21] N. C. Menicucci, S. J. Olson, and G. J. Milburn, *New J. Phys.* **12**, 095019 (2010).
- [22] C. Roos, *Controlling the quantum state of trapped ions*, Ph.D. thesis, Universität Innsbruck (2000).
- [23] S. C. Doret, J. M. Amini, K. Wright, C. Volin, T. Killian, A. Ozakin, D. Denison, H. Hayden, C.-S. Pai, R. E. Slusher, and A. W. Harter, *New J. Phys.* **14**, 073012 (2012).
- [24] D. Leibfried, R. Blatt, C. Monroe, and D. Wineland, *Rev. Mod. Phys.* **75**, 281 (2003).
- [25] D. J. Berkeland, J. D. Miller, J. C. Bergquist, W. M. Itano, and D. J. Wineland, *J. Appl. Phys.* **83**, 5025 (1998).
- [26] N. D. Guise, S. D. Fallek, K. E. Stevens, K. R. Brown, C. Volin, A. W. Harter, J. M. Amini, R. E. Higashi, S. T. Lu, H. M. Chanhvongsak, T. A. Nguyen, M. S. Marcus, T. R. Ohnstein, and D. W. Youngner, *J. Appl. Phys.* **117**, 174901 (2015).